# Initial transients in the symmetric model for directional solidification

Raúl Benítez and Laureano Ramírez-Piscina

Departament de Física Aplicada. Universitat Politècnica de Catalunya. Av. Dr. Marañón 44, E-08028 Barcelona. Spain.

**Abstract.** We study the initial transient during the directional solidification of a dilute mixture in the symmetrical constant-gap approximation. We perform phase-field simulations of the transient recoil stages and compare the results with predictions obtained from the sharp-interface model. In particular, we focus in the evolution of the front position and of the transient dispersion relation, obtaining quantitative agreement between theory and simulations. Results are applied to the destabilization of the front by fluctuations.

## 1 Introduction

The selection of a dendritic pattern during the directional solidification of a dilute binary alloy is a complex problem which depends on initial conditions[1], and in particular on the first wavelengths that appear in the destabilization of the planar front induced by fluctuations[2,3]. Recent work has focused in the importance of internal fluctuations in solidification patterns [4,5]. Quantitative agreement with experiments has only been obtained for the solidification of pure substances, whereas in solutal growth the origin itself of the fluctuations is still an open problem [6,7]. The aim of this work is to use phase-field techniques to study the effects of transients and fluctuations in the selection problem of directional solidification. For this objective we have performed a quantitative comparison between phase-field simulations and predictions for the sharp-interface model.

## 2 The sharp-interface model

In a directional solidification experiment, a thermal gradient $G\hat{\mathbf{z}}$ is moved in the $\tilde{z}$ direction along the sample at constant pulling velocity $V\hat{\mathbf{z}}$. Provided the sample is thin, we take the system as 2D and describe the interface position in the moving frame of the gradient by $\tilde{z} = \tilde{\xi}(\tilde{\boldsymbol{\rho}}, \tilde{t})$, where $\tilde{\boldsymbol{\rho}} = \tilde{x}\hat{\mathbf{x}} + \tilde{y}\hat{\mathbf{y}}$. The solid phase is located in the region where $\tilde{z} < \tilde{\xi}$, and the liquid where $\tilde{z} > \tilde{\xi}$. We will consider the particular case of symmetric directional solidification, which assumes the same solute diffusivity $D$ in both phases. We introduce diffusion length $l = D/V$ and time $\tau = D/V^2$ to scale variables as $\boldsymbol{r} = \tilde{\boldsymbol{r}}/l$ and $t = \tilde{t}/\tau$. We also introduce a diffusive field in each phase $u_i(\boldsymbol{r}, t) = \frac{C_i - C_\infty}{\Delta C_0}$ (i=1 solid, i=2 liquid), where $C_i$ is the solute concentration, $C_\infty$ the concentration far

away from the solid-liquid interface, and $\Delta C_0 = [C_2 - C_1]_{int}$ the concentration jump across the interface. In the moving frame and in reduced variables, the fields $u_i$ evolve according to the diffusion equation

$$(\frac{\partial}{\partial t} - \frac{\partial}{\partial z} - \nabla^2) u_i(\boldsymbol{r}, t) = 0. \tag{1}$$

The diffusion fields $u_i$ must satisfy some moving boundary conditions at the interface position which can be written as

$$[u_1 - u_2]_{int} = -1 \tag{2}$$

$$u_2|_{int} = 1 - \frac{l}{l_T}\xi + \frac{d_0}{l}\kappa \tag{3}$$

$$\hat{\mathbf{n}} \cdot \left[\boldsymbol{\nabla} u_1 - \boldsymbol{\nabla} u_2\right]_{int} = -n_z(1 + \dot{\xi}) \tag{4}$$

Equations (1-4) define the so called sharp-interface description of the symmetric directional solidification problem. Equation (2) relates solute concentrations at both sides of the interface. We have assumed the additional approximation of having a constant concentration jump across the interface. This particular assumption is equivalent to suppose that the mixture has parallel solid and liquid branches in the $T(C)$ coexistence diagram, which is valid only for liquid crystals and alloys with a partition coefficient close to 1. Eq. (3) is the Gibbs-Thompson equation (local equilibrium at the interface). In this relation $l_T = |m_L|\Delta C_0/G$ is a thermal length imposed by the temperature gradient, and $d_0$ is the capillary length. Eq. (4) describes the solute conservation across the interface, and $\hat{\boldsymbol{n}}$ represents a normal unitary vector pointing to the liquid. Using Green's function techniques [8], it is possible to derive a closed integral expression for $u_i$ at each side of the interface. Introducing the notation $p = (\boldsymbol{\rho}, z, t)$, $p_S = (\boldsymbol{\rho}, \xi, t)$, the concentration at the interface verifies

$$\begin{aligned} \tfrac{1}{2}u_i(p_S) = (-)^i \Big( & \int_{\xi(\boldsymbol{\rho},t_0)}^{(-)^i\infty} d\boldsymbol{r'} \cdot G_i(p_S, \boldsymbol{r'}, t_0) \cdot u_i(\boldsymbol{r'}, t_0) \\ & - \int_{t_0}^{t} dt' \int d\boldsymbol{\rho'} \cdot [1 + \dot{\xi}(\boldsymbol{\rho'}, t')] \cdot u_i(p'_S) \cdot G(p_S, p'_S) \\ & - \int_{t_0}^{t} dt' \int dS' \hat{\mathbf{n}}' \cdot [G_i(p_S, p'_S)\boldsymbol{\nabla}' u_i(p'_S) - u_i(p'_S)\boldsymbol{\nabla}' G_i(p_S, p_{S'})] \Big) \end{aligned} \tag{5}$$

where $G_i(p, p')$ is the retarded Green's function of the diffusion problem

$$G(p, p') = \frac{\theta(t - t')}{[4\pi(t - t')]^{\frac{3}{2}}} \exp\left\{ -\frac{(\boldsymbol{\rho} - \boldsymbol{\rho'})^2 + (z - z' + t - t')^2}{4(t - t')} \right\}. \tag{6}$$

Summing Eq. (5) over $i = 1, 2$, and using the moving boundary conditions Eqs. (2-4), an integro-differential equation can be obtained for the interface position during the transient

$$\begin{aligned} \frac{l}{l_T}\xi(\boldsymbol{\rho}, t_0) = & -\int_{-\infty}^{\xi(\boldsymbol{\rho},t_0)} d\boldsymbol{r'} G(p_s; \boldsymbol{r'}, t_0) u_1(\boldsymbol{r'}, t_0) - \int_{\xi(\boldsymbol{\rho},t_0)}^{\infty} d\boldsymbol{r'} G(p_s; \boldsymbol{r'}, t_0) u_2(\boldsymbol{r'}, t_0) + \\ & \int_{t_0}^{t} dt' \int d\boldsymbol{\rho'} (1 + \dot{\xi}(\boldsymbol{\rho'}, t)) G(p_s, p'_s) + \tfrac{1}{2}(1 + erf(\tfrac{\xi(\boldsymbol{\rho},t) - \xi(\boldsymbol{\rho},t_0) + t}{2\sqrt{t}})) \end{aligned} \tag{7}$$

where $\xi = 0$ stands for the steady position of an unperturbed planar interface. Note that Eq. (7) includes transients from the initial condition at $t_0$.

The next step is to perform a linear stability analysis of the problem to obtain a transient dispersion relation describing the time evolution of a sinusoidal modulation with wavevector $kl$. Within an adiabatic approximation [2,3] we derive the growth ratio of the mode as

$$\omega(kl,t) = \frac{l}{l_T}\dot{\xi} - (1+\dot{\xi})^2 + q_2(1+\dot{\xi}) - (q_1+q_2)\left[\frac{l}{l_T} + \frac{d_0}{l}(kl)^2\right], \quad (8)$$

where

$$q_\alpha = \tfrac{(-1)^\alpha}{2}(1+\dot{\xi}) + \sqrt{\tfrac{1}{4}(1+\dot{\xi})^2 + (kl)^2 + \omega(kl,t)}. \quad (9)$$

Therefore the prediction of the transient dispersion relation consists of two steps. Firstly the numerical resolution of Eq. (7) for a planar interface is performed by a Newton-Raphson method, yielding the transient front position $\xi(t)$. This function is then introduced into Eq. (8) to obtain $\omega(kl,t)$ in this adiabatic approximation.

## 3 The phase-field model

In the last few years, phase-field models have become a quantitative technique to numerically simulate solidification phenomena [9]. This method introduce a continue variable (the phase-field) $\phi(\boldsymbol{r},t)$ which takes different constant values in the solid and liquid phases, and that localizes the solid-liquid interface in a diffuse region of thickness $W$. This field is coupled with the solute diffusion field, and the parameters are chosen in such a way that in the limit $\varepsilon = W/l \to 0$ the interface dynamics recovers the behavior described by the sharp-interface model. We will use a phase-field model introduced by Karma et. al. [10] for symmetric directional alloy solidification with constant concentration gap. For isotropic solidification with no kinetic dynamics, the equations in reduced variables take the form

$$\tfrac{a_1 a_2}{d_0/l}\varepsilon^3\partial_t\phi = \varepsilon^2\nabla^2\phi + (1-\phi^2)(\phi - \varepsilon\tfrac{a_1}{d_0/l}(1-\phi^2)(u + \tfrac{z-t}{l_T/l})) \quad (10)$$

$$\partial_t u = \nabla^2 u + \tfrac{1}{2}\partial_t\phi. \quad (11)$$

In this model, $a_1 = \frac{5\sqrt{2}}{8}$, $a_2 = 0.6267$ are integral constants obtained when performing a thin-interface limit [9]. Note that the equation for the phase-field evolution contains three parameters: two main control parameters coming from the sharp-interface model ($l_T/l$ and $d_0/l$), and the model-specific parameter $\varepsilon$.

## 4 Results and discussion

We will consider the transient from the rest, i.e. for an initial condition at $t_0 = 0$ consisting of an equilibrium solid-liquid planar interface located at $\xi(t = 0) = l_T/l$. In this case $C_1(\boldsymbol{r}, 0) = C_\infty - \Delta C_0$ ($u_1(\boldsymbol{r}, 0) = -1$), and $C_2(\boldsymbol{r}, 0) = C_\infty$ ($u_2(\boldsymbol{r}, 0) = 0$).That corresponds to taking $u(\boldsymbol{r}, 0) = -1$ as initial condition for the phase-field model. Trying to mimic a real experiment, we consider here that at $t = 0$ the pulling velocity suddenly takes the final value V (1 in scaled variables).

We perform numerical integration of the phase-field Eqs. (10,11) with an explicit finite-differences scheme with $\Delta x = 0.8$ and $\Delta t = 0.08$ . We first study the 1D dynamical evolution during the transient, comparing the results with the sharp-interface predictions. Fig. 1 presents the front position for two different values of the control parameter $l_T/l = 12.5$ and 2.5. For each case, we compare simulations for three different values of $\varepsilon$ ($\varepsilon = 0.5$, $\varepsilon = 0.25$ and $\varepsilon = 0.125$) with the front position obtained with direct resolution of the integral equation (7). Convergence to the sharp-interface limit can be observed as $\varepsilon$ decreases, and good agreement is found for a value of $\varepsilon = 0.125$.

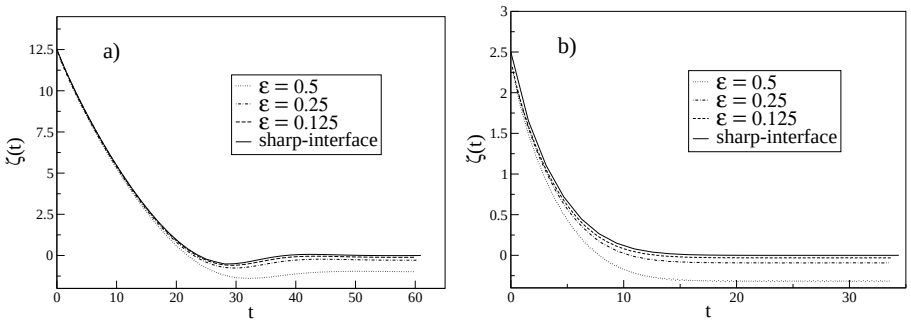


**Fig. 1.** Evolution of the interface position during the transient for (a) $l_T/l = 12.5$ and (b) $l_T/l = 2.5$, and convergence to the sharp-interface as $\varepsilon \to 0$.

We now estimate the transient dispersion relation $\omega(kl, t)$ from phase-field simulations and compare it with the sharp interface prediction of Eqs. (8, 9). To this end we simulate for each desired value of $t$ a (planar) 1D interface evolving from $t_0 = 0$ to $t$. At that moment we introduce a sinusoidal interface perturbation with wavevector $kl$, and continue the simulation in 2D. The spectral analysis of the front allows us to locate the regime where the mode evolution is linear. This is represented in Fig. 2.a, where three definite regions can be observed. From the linear region the value of the transient growth rate $\omega(kl, t)$ is calculated. Fig. 2.b shows the growth rate at different times obtained for two different modes $kl = 1.25$ and $kl = 2.5$ in the case of

$l_T/l = 12.5$ and $d_0/l = 0.06923$. Quantitative agreement is observed for all times.

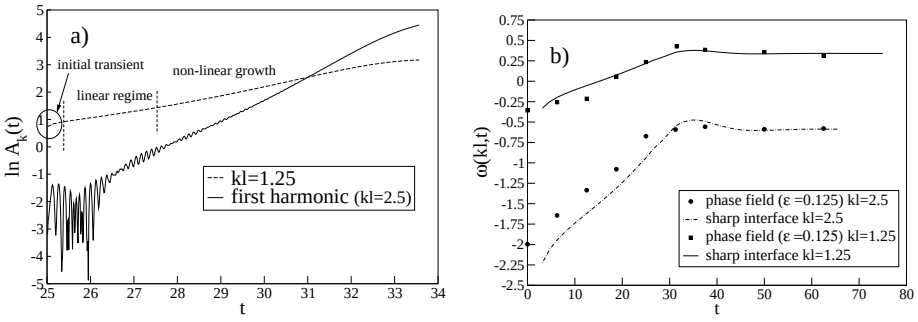


**Fig. 2.** a) Localization of the linear growth regime of the mode $kl = 1.25$. b) Time evolution of two different modes $kl = 1.25$ and $kl = 2.5$ for $l_T/l = 12.5$.

In the last part of this work we have introduced internal fluctuations in the diffusion equation of the phase-field by following the formalism introduced in Ref. [11]. In simulations the growth of a range of wavelengths can be observed until a selected mode dominates. The spectral analysis of the front reveals a good agreement during the linear regime between the growth of each mode and the transient dispersion relation predicted by the sharp interface model. In Fig. 3 we present the amplitude of one of the modes ($kl = 2.5$, $l_T/l = 12.5$) averaged for 15 different noise realizations. The agreement is quite good in the regime with positive $\omega$ (i.e. where an increasing $A_k(t)$ is predicted).

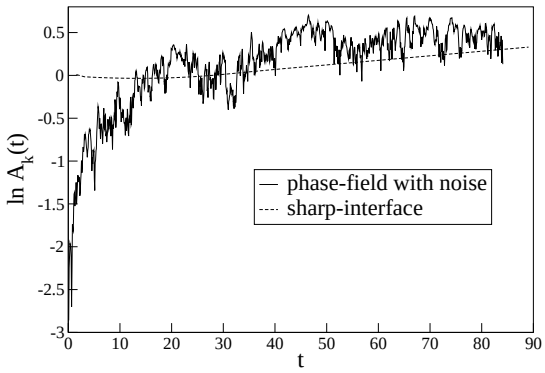


**Fig. 3.** Time evolution of the mode $kl = 2.5$ ($l_T/l = 12.5$) with the phase-field with noise, and comparison with the sharp-interface prediction.

## 5 Concluding remarks

In this paper we have studied the initial stages of a directional solidification experiment in the context of the symmetric model. We have presented predictions for the transient recoil of the sharp interface model and for the transient dispersion relation by using an adiabatic approximation. We have performed phase field simulations of this initial regime. Simulations quantitatively agree with theoretical calculations. In particular the analysis of the evolution of single modes and of fronts with fluctuations, both from theory and from simulations, should be of relevance in the dendritic selection problem. Work in progress [12] are extending these results to the one-side model and to the Langevin formalism for the modes of Ref. [2].

We acknowledge financial support from Dirección General de Investigación Científica y Técnica (Spain) (Project BFM2000-0624-C03-02) and Comissionat per a Universitats i Recerca (Spain) (Project 2001SGR 00221).

## References

1. Warren, J.A., Langer, J.S.: Stability of dendritic spacings. Phys. Rev. E **42** (1990) 3518–3525
2. Warren, J.A., Langer, J.S.: Prediction of dendritic spacings in a directional-solidification experiment. Phys. Rev. E **47** (1993) 2701–2712
3. Caroli, B., Caroli, C., Ramírez-Piscina, L.: Initial front transients in directional solidification of thin samples of dilute alloys. J. Cryst. Growth **132** (1993) 377–388
4. Brener, E., Temkin, D.: Noise-induced sidebranching in the three-dimensional nonaxissymmetric dendritic growth. Phys. Rev. E **51** (1995) 351–359.
5. Pocheau, A., Georgelin, M.: Validation criterion for noise-induced mechanism of sidebranching in directional solidification. Eur. Phys. J. B. **21** (2001) 229–240
6. Losert, W., Shi, B.Q., Cummins, H.Z.: Proc. Natl. Acad. Sci. USA **95** (1998) 439–442
7. González-Cinca, R., Ramírez-Piscina, L., Casademunt, J., Hernández- Machado, A.: Noise-induced sidebranching in a phase-field model for solidification. Phys. Rev. E **63** (2001) 051602
8. Caroli, B., Caroli, C., Roulet, R.: On the linear stability of needle crystals: evolution of a Zel'dovich localized front deformation. J. Phys. France **48** (1987) 1423–1437
9. Karma, A., Rappel, W.J. : Quantitative phase-field modeling of dendritic growth in two and three dimensions. Phys. Rev. E **57** (1998) 4323–4349
10. Losert, W., Stillman, D.A., Cummins, H.Z., Kopczynski, P., Rappel, W.J., Karma, A.: Selection of doublet cellular patterns in directional solidification through spatially periodic perturbations. Phys. Rev. E **58** (1998) 7492–7506
11. Karma, A., Rappel, J.W.: Phase-field model of dendritic sidebranching with thermal noise. Phys. Rev. E **60** (1999) 3614–3625
12. Benítez, R., Ramírez-Piscina, L.: In preparation.